Experimental testing of 3D printed polymeric heat exchangers

Experimental testing of 3D printed polymeric heat exchangers

Experimental testing of 3D printed polymeric heat exchangers

L Fontana[1], P Minetola[1], F Calignano[1], L Iuliano[1], M S Khandpur and V Stiuso[1]

[1] Dept. Management and Production Engineering (DIGEP), Politecnico di Torino, Corso Duca degli Abruzzi 24, 10129 - Torino, Italy

luca.fontana@polito.it

Abstract. Unlike conventional manufacturing technologies, additive manufacturing and 3D printing empower engineers with much more design freedom. Heat exchangers with complex internal channels or lattice structures can be designed for layerwise manufacturing by maximizing the surface to volume ratio. Low-weight polymeric heat exchangers are employed in aviation and aerospace applications. For increasing the thermal performance of polymers, additives can be used such as graphene. In this study, a Grafylon filament is used for the production of a simple heat exchanger by 3D printing. The heat exchanger is composed of two external shells and an interior duct with a two-stage 45-degree bend. For watertight purposes, the duct is manufactured by selective laser sintering of polyamide powder. Two replicas of the shells are fabricated by 3D printing of Grafylon and acrylonitrile butadiene styrene (ABS) respectively. The thermal performance of the two materials is experimentally tested and compared also to numerical simulations. The results of the study show that the Grafylon filament provides enhanced thermal performance to 3D printed heat exchangers of polymeric material.

1. Introduction

Additive manufacturing (AM) and 3D Printing (3DP) refer to a group of layerwise production technologies [1] that are revolutionizing manufacturing in different industrial sectors within the digital paradigm of the Industry 4.0 framework [2, 3]. The design freedom of layerwise manufacturing allows engineers to create hollow parts with complex internal channels or lattice structures to be used in a wide range of applications. In the energy sector, this advantage is exploited to maximize the surface to volume ratio for enhanced performance of heat exchangers [4-8]. Many additive manufacturing techniques allow producing complex heat exchangers as a single component, without the need for assembling or joining operations [9].

Polymeric heat exchangers have recently received the attention and interest of the avionic and aerospace sectors due to their low weight, and resistance to corrosion and chemicals [10]. To this aim, new materials with better thermal properties, like Graphene [11] are being experimented. In recent years, attempts have been made to use graphene, or its composites, as a raw material or charge in filaments for 3D printing, that is for the Fused Deposition Modelling (FDM) or Freeform Filament Fabrication (FFF) processes [12].

However, as-built 3D printed parts are not waterproof because the adhesion between the layers leaves small voids or gaps for leakages of low viscosity fluids. This problem is normally solved through post-processing and infiltration of the as-built 3D printed part with a filler. For example, Nano-Seal is a modified silica nano-composite material that creates a protective barrier for all exterior surfaces. Nevertheless, infiltration requires long processing times (hours) and the amount of filler deposited on the surface of complex internal holes cannot be easily controlled.

To test for the thermal performance of graphene charged 3D printing filaments, in this work a simple small heat exchanger is manufactured and tested. To overcome sealing issues of 3D printed parts while avoiding the infiltration treatment, the duct of the heat exchanger was manufactured by selective laser sintering (SLS). In SLS, polymeric powders are selectively melted by a laser source layer after layer. SLS provides full material density and leakage-proof surfaces to fluids. The SLS duct of polyamide 12 (PA12) is then enclosed within two square shells printed using a graphene-charged polylactic acid (PLA) filament. The thermal performance of this material is compared to that of a standard acrylonitrile-butadiene-styrene (ABS) filament, that is used to print another replica of the heat exchanger shells.

The comparison is carried out by numerical and experimental analyses. Thermal simulations are run by means of Solidworks Flow Simulation assuming thermal conductivity values of the different materials from the supplier datasheet. The variation over time of the temperature of the heat exchanger is predicted in operative conditions using the numerical model. Finally, experimental measurements are carried out using a thermal camera to validate the results of the simulations and compare the performance of the graphene-charged filament to the ABS one.

2. Materials and methods

The heat exchanger was designed considering a two-stage 45-degree duct (figure 1). Two replicas of the heat exchanger were 3D printed and tested.

2.1. Production of the heat exchangers

For the abovementioned watertight purposes, the duct was fabricated by SLS with 0.10 mm layer thickness of EOS PA2200, a polyamide 12 powder, using an EOS Formiga Velocis system. The duct has an internal diameter of 5 mm and a wall thickness of 3 mm. The outer shells for the casing and plates of the heat exchanger were produced using an open A4v3 3D printer by the Italian company 3ntr. For one replica of the shells, the 3D printer was fed with a 2.85 mm red ABS filament by Filoalfa (figure 2), while for the second replica a Grafylon filament by Filoalfa was used. Grafylon is the result of a collaboration between Filoalfa and Directa Plus companies and the filament contains Graphene Plus, that is a nanomaterial made up of Pristine Graphene Nanoplatelets (GNPs). The graphene charge conveys a characteristic shiny dark gray colour to the 3D printed part (figure 3). When compared to traditional PLA, the Grafylon filament has enhanced thermal and mechanical performance, with higher elastic module (+34%), tensile strength (+ 23%) and elongation at break (+ 28%).

The two halves of the heat exchanger casing have overall dimensions of 70 x 70 and are 8 mm thick. They were 3D printed with 0.20 mm layer thickness and 50% infill. The external side is flat, whereas their internal surface is shaped to correctly match the form of the PA duct. After 3D printing, each couple of shells of ABS (figure 2) or Grafylon (figure 3) is assembled around the duct with two bolted joints. The bolted joints are placed far from the duct and close to the opposite corners of the shells.

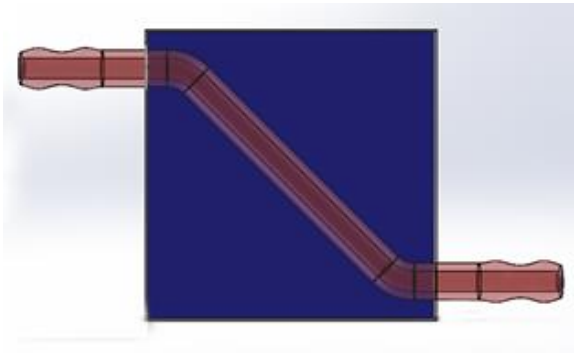

Figure 1. CAD model of the 3D printed multimaterial heat exchanger.

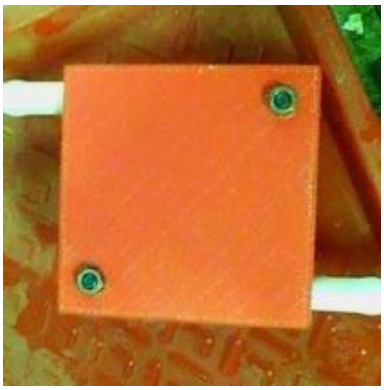

Figure 2. 3D printed heat exchanger with ABS casing and PA12 duct.

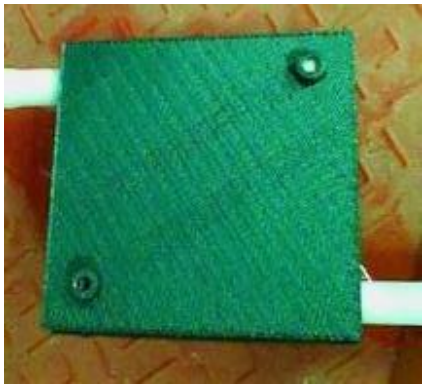

Figure 3. 3D printed heat exchanger with Grafylon casing and PA12 duct.

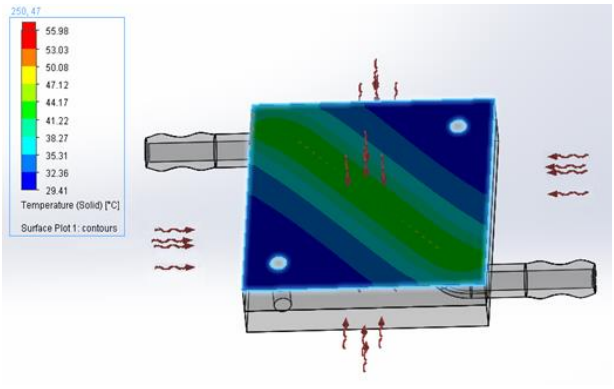

Figure 4. Thermal simulation model in Solidwork Flow Simulation module.

2.2. Simulation model

The presence of connection elements is not considered in the simplified simulation model of the heat exchanger that was implemented in Solidworks software (figure 4). In the numerical model all materials were assumed to have an isotropic behaviour for the thermal conductivity. The material properties for the duct and shells were set as shown in Table 1.

Table 1. Material properties for the simulation model.

Property	PA12 duct	ABS shell	Grafylon shell
Volume (cm^3)	6.82	36.00	36.00
Part weight (gr)	6.91	30.10	33.30
Real part density (gr/cm^3)	1.013	0.836	0.925
Specific heat J/(kg·K)	1185	1080	1800

The value of the specific heat was taken from the material datasheet, while the material density was computed as the ratio between the weight of the 3D printed part and the volume of the CAD model. Therefore the material density considers the effect of the 50% infill for the ABS and Grafylon plates.

The weight of the parts was measured with a 1000HR-CM balance by Gibertini with a resolution of 0.01 g. In the numerical analyses, heat conduction inside the material and radiation towards the external environment were considered with the heat exchange coefficient between the external surface of the shells and the air equal to 10 W/(m2·K).

Water was used as a heat transfer fluid. Its flow rate and temperature together with the value of the air temperature and initial temperature of the heat exchanger (table 2) were set as input for the simulation of the heat transfer over 600 seconds.

Table 2. Experimental conditions for the simulation and testing of the heat exchangers.

Heat exchanger materials	Water flow rate	Water temperature	Air Temperature	Initial temperature of the heat exchanger
ABS with PA12 duct	0.05 l/s	56.0 °C	31.8 °C	30.7 °C
Grafylon with PA12 duct	0.05 l/s	55.3 °C	31.3 °C	30.5 °C

Several simulations were run to account for the range of thermal conductivity indicated by Filoalfa in the datasheet of the two 3D printing materials. Four simulations were used for the ABS whose thermal conductivity was varied between 0.12 and 0.21 W/(m·K) with increments of 0.03 W/(m·K). In the case of the Grafylon, six simulations were run to cover a range between 0.19 and 0.38 W/(m·K) for the thermal conductivity with increments of 0.04 W/(m·K). For the PA2200 material, the thermal conductivity was set to 0.23 W/(m·K).

2.3. Experimental tests

An electric water pump of 3-meter head with a maximum flow rate of 1500 l/h was used to pump the water into the heat exchanger from a reservoir. The experimental conditions were slightly different for the two heat exchangers of ABS and Grafylon material as detailed in table 2. The temperatures were measured on thermal images captured using an E4 thermal camera by FLIR with a measuring range from –20°C to +250°C and a measurement uncertainty of ±2% of reading. The values of the minimum (T_{min}), average (T_{avg}), and maximum (T_{max}) temperatures of the upper surface of the heat exchangers were recorded after 180, 300, and 600 seconds from the start of the pump for hot water circulation. The experimental values of these temperatures were then compared to the ones of the numerical simulations.

3. Results and comparison

The results of the experimental tests and those of the thermal simulations are summarized in figure 5 and figure 6 for the ABS heat exchanger and the Grafylon one respectively. The uncertainty of the experimental measurement with the FLIR E4 camera is represented by the error bars and colored band. In general, there is a very good correspondence between the experimental values of the temperatures and the simulated ones.

The minimum temperature T_{min} is scarcely affected by the value of the thermal conductivity of the ABS or Grafylon material. The minimum temperature of the heat exchanger remains close to the room temperature (air temperature in table 2) during the test. The real average temperature T_{avg} is overestimated by the simulations run with a higher value of the thermal conductivity of the 3D printing material. This difference can be attributed to the simplified simulation model that considers the heat exchanger only but not the complete hydraulic circuit. Therefore the heat dissipated in the tank, pump, and connecting hoses is neglected by the numerical simulations.

For the ABS heat exchanger (figure 5), the comparison of maximum temperature T_{max} between the experimental results and the numerical ones is similar to that of the average temperature T_{avg}. In the case of the Grafylon replica (figure 6), after 180 seconds the real maximum temperature T_{max} exceeds the value estimated by the simulations independently of the assumed thermal conductivity level.

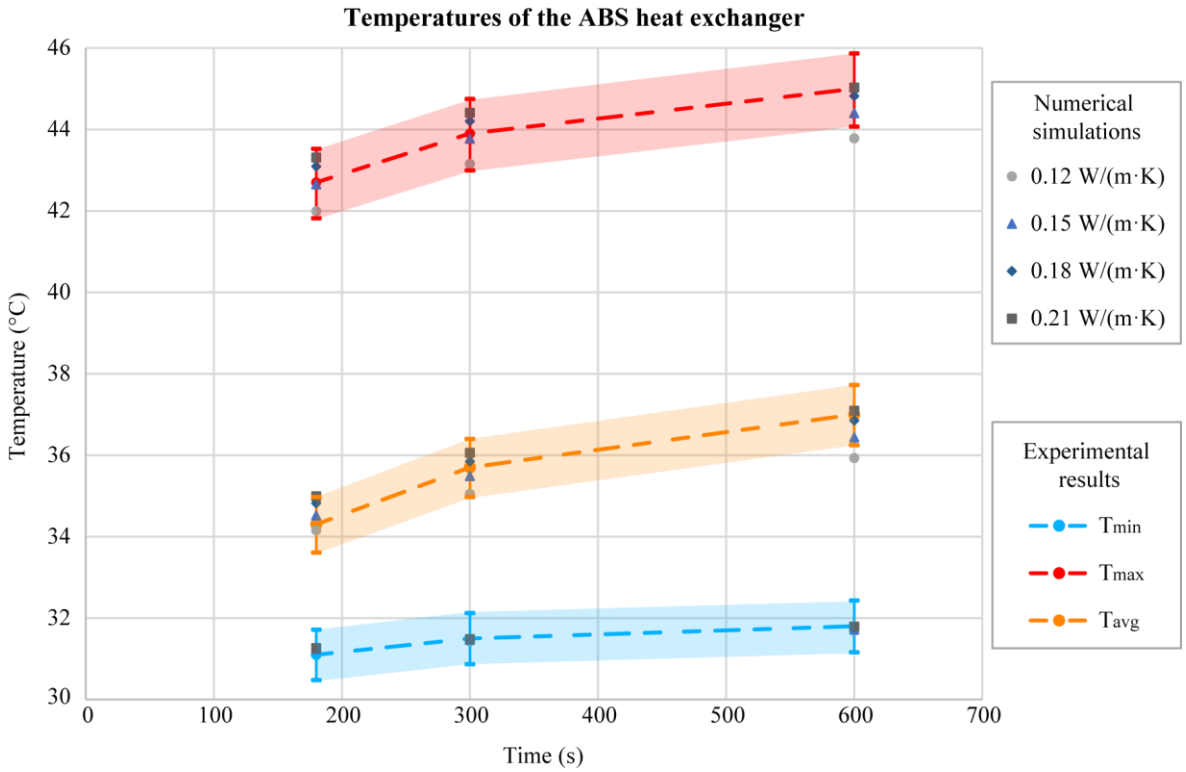

Figure 5. Comparison of experimental and numerical results for the ABS heat exchanger.

This result might suggest that the dynamics of the heat transfer at the starting of the experimental test is not as fast as the simulation predicted under ideal condition. The Grafylon material is not dissipated all the initial heat conveyed by the hot water and the maximum temperature T_{max} of the heat is above the simulated values.

As the experimental test continues, the real maximum temperature T_{max} for the Grafylon heat exchanger is very close to the numerical values predicted with the highest thermal conductivity of 0.38 W/(m·K). Over the 600 seconds, no clear difference could be observed between the levels of the considered temperatures for the ABS replicas and the Grafylon one.

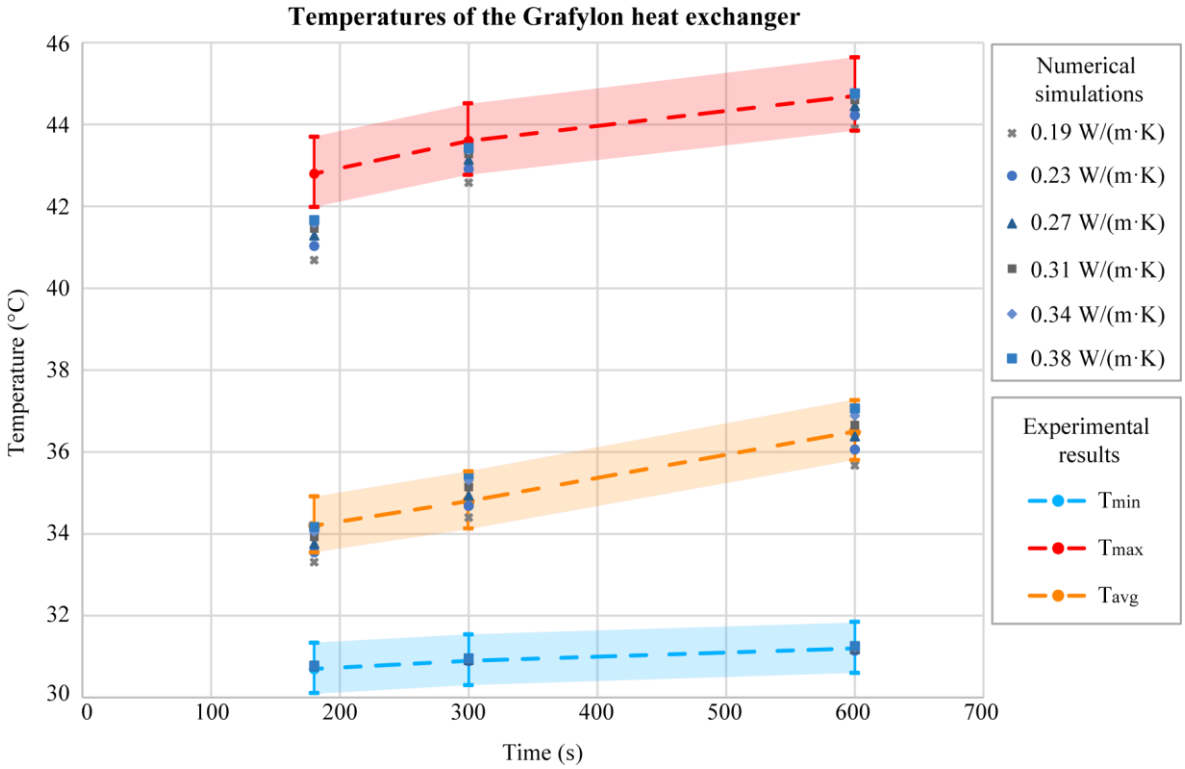

Figure 6. Comparison of experimental and numerical results for the Grafylon heat exchanger.

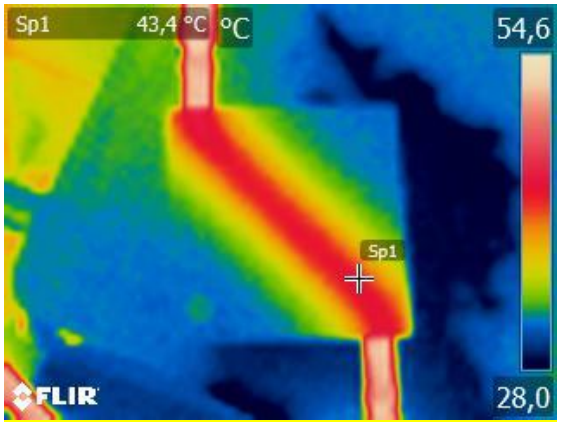

Figure 7. Thermal image of ABS heat exchanger after 600s from the start of the pump.

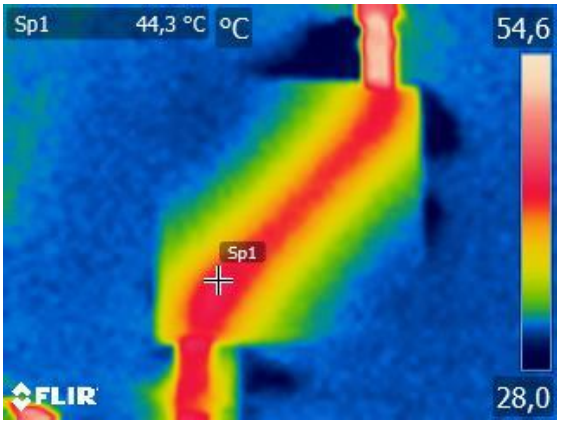

Figure 8. Thermal image of the Grafylon heat exchanger after 600s from the start of the pump.

Therefore, despite the higher thermal conductivity values of the graphene-charged PLA, as also confirmed by the simulations, similar temperatures are reached in the two heat-exchangers.

Nevertheless, the images of the thermal camera show that the surface of the Grafylon replica dissipates more heat as the bolted corners that are far from the heat source of the hot water in the PA12 duct.

By comparing the thermal image of the ABS replica (figure 7) to that of the Grafylon heat exchanger (figure 8) after 600 seconds, it is possible to distinguish the shape and presence of the metal bolts that join the two ABS shells around the duct. In the infrared image of the ABS heat exchanger, the bolts are visible because their metallic material has a higher thermal conductivity than the polymeric shell. The bolts are heated by the hot water and the ABS casing is not able to dissipate their heat as well as the Grafylon material does.

4. Conclusions

The development of new materials for 3D printing will be the key to widen the range of applications for this technology. In this paper, the thermal performance of a graphene-charged PLA filament was compared to the one of a conventional ABS filament.

One replica of a simple heat exchanger was 3D printed by combining SLS and FDM techniques to compare the performance of the two filaments. Numerical simulations were also run to predict the results of the experimental tests. The measures of real temperatures using a thermal camera were in good agreement with the simulation results.

Under the testing conditions, slightly better heat dissipation capacity was observed for the 3D printed filament with the graphene charge. However, future studies should consider the design freedom of additive manufacturing for combining more complex shapes for the heat exchanger with the enhanced thermal conductivity of the Grafylon material.

Form the sustainability perspective, different filling strategies and percentages in 3D printing of polymeric heat-exchangers should be considered to minimize material consumption while maximizing the surface-to-volume ratio. Finally, the development of nanofilled technopolymers for 3D printing would be interesting for promising heat-transfer applications in the aerospace sector.

Acknowledgments

The authors gratefully acknowledge Mr. Loris Lombardo, MSc. student in Energetic Engineering of Politecnico di Torino, for his assistance with the development of the simulation model and experimental testing of the heat exchangers.

References

[1] Calignano F *et al.* 2017 *Proc. IEEE* **105**(4) 593-612
[2] Dilberoglu U M, Gharehpapagh B, Yaman U and Dolen M 2017 *Procedia Manuf.* **11**, 545-54
[3] Haleem A and Javaid M 2019 *J. Ind. Integr. Manag.*, **4**(04) 1930001
[4] Arie M A, Shooshtari A H, Dessiatoun S V and Ohadi M M 2016 *Heat Transfer Summer Conf.* 50336 (Washington, DC: American Society of Mechanical Engineers) p V002T22A002
[5] Saltzman D, Bichnevicius M, Lynch S, Simpson T W, Reutzel E W, Dickman C and Martukanitz R 2018 *Appl. Therm. Eng.* **138** 254-63
[6] Gerstler W D and Erno D 2017 *2017 16th IEEE Intersociety Conference on Thermal and Thermomechanical Phenomena in Electronic Systems (ITherm)* (Orlando: IEEE) pp 624-33
[7] Lebaal N, SettaR A, Roth S and Gomes S 2020 *Mech. Adv. Matl. Struct.* 1-9
[8] Zhang X, Arie M A, Deisenroth D C, Shooshtari A, Dessiatoun S and Ohadi M 2015 *9th Minsk Int. Seminar on Heat Pipes, Heat Pumps, Refrigerators, Power Sources* (Minsk) pp 7-10
[9] Keramati H, Battaglia F, Arie M A, Singer F and Ohadi M M 2019 *2019 18th IEEE Intersociety Conf. on Thermal and Thermomechanical Phenomena in Electronic Systems (ITherm)* (Las Vegas: IEEE) pp 423-29
[10] Collins I L, Weibel J A, Pan L and Garimella S V 2019 *Int. J. Heat Mass Tran.* **131** 1174-83
[11] Shahil K M and Balandin A A 2012 *Solid State Commun* **152**(15) 1331-40
[12] Foster C W, Down M P, Zhang Y, Ji X, Rowley-Neale S J, Smith G C, Kelly P J and Banks C E 2017 *Scientific Report* **7**(1) 1